Radial Basis Function Neural Network for Power System Transient Energy Margin Estimation

Ali Karami†

Abstract – This paper presents a method for estimating the transient stability status of the power system using radial basis function (RBF) neural network with a fast hybrid training approach. A normalized transient energy margin (ΔV_n) has been obtained by the potential energy boundary surface (PEBS) method along with a time-domain simulation technique, and is used as an output of the RBF neural network. The RBF neural network is then trained to map the operating conditions of the power system to the ΔV_n, which provides a measure of the transient stability of the power system. The proposed approach has been successfully applied to the 10-machine 39-bus New England test system, and the results are given.

Keywords: Energy margin, PEBS method, Radial basis function neural network, Transient stability

1. Introduction

Power system stability denotes the ability of an electric power system, for a given initial operating conditions, to regain a sate of equilibrium after being subjected to a physical disturbance, with most system variables bounded so that system integrity is preserved [1]. Power system stability is broadly classified as rotor angle stability, frequency stability, and voltage stability [2]. Rotor angle stability is concerned with small signal stability analysis and transient stability analysis (TSA). The ability of power systems of surviving to a large disturbance through a short-term period (e.g., up to several seconds) following the disturbance is referred as transient stability [3].

There are common methods for TSA: one of them is based on the time-domain simulation technique [4]-[5], and the others are either based on the transient energy function (TEF) method [6]-[7], or the extended equal area criterion (EEAC) [8]-[9]. The time-domain simulation technique is the most accurate method for assessing the power systems transient stability. This method has the capability of using detailed models of the synchronous generators and its controllers [4]-[5]. However, one of the disadvantages of this method is the CPU time in real-time and on-line applications.

Neural networks (NNs) have been proposed as an alternative method for TSA problem by many authors since Sobajic and Pao [10] explored the capability of the NNs for TSA. Sobajic and Pao used NNs for prediction of the critical clearing time (t_{cr}) for a small test power system. Djukanovic et al. [11] used individual energy function normalized by the critical value of global energy function evaluated at fault clearing time to predict energy margin and stability. Pao and Sobajic [12] proposed a combined usage of unsupervised and supervised learning for TSA. Fast pattern recognition and classification of dynamic security states were reported by Zhou et al. [13]. A feed-forward NN was trained using energy margin and unstable equilibrium point angles of advanced generators as the inputs with power system vulnerability as the output. Hobsen and Allen [14] reported that the NNs have difficulty in returning consistent accurate answers under varying network conditions. Aboytes and Ramirez [15] used NNs to predict stability of a 53 generators system. Bahbah and Grigis [16] used the recurrent radial basis function (RBF) and the multi-layer perceptron (MLP) NNs for dynamic system modeling, the generators' angles and angular velocities prediction for TSA.

Selection of the neural networks inputs is an important factor in a successful use of the NNs for the TSA. In all the above-mentioned papers, pre-fault variables and variables during fault have been used as the inputs for the NNs. The main problem of these papers is that the determination of some inputs of the NNs is a time-consuming task. Because, we must use some supplementary tools such as the load-flow and/or transient stability software for the neural networks inputs determination. In addition, most of the published work in this area utilizes the MLP model based on back propagation (BP) algorithm, which usually suffers from local minima and over-fitting problems.

The main objective of the present investigation is to propose an RBF neural network based approach for on-line transient stability analysis through estimation of a normalized transient energy margin (ΔV_n). The main idea is that for a particular fault scenario, the ΔV_n is a

† Faculty of Engineering, University of Guilan, Rasht, Iran.
(karami_al@yahoo.com &karami_s@guilan.ac.ir)
Received 26 June, 2008 ; Accepted 2 October, 2008

function of only pre-fault system operating point, which can be adequately characterized by a proper set of directly measurable operating conditions (features) in the pre-fault situations. Therefore, an RBF neural network, which is well known for its universal approximation capabilities [17], can be employed to approximate the function.

For obtaining the ΔV_n training or testing data patterns quickly, the Potential Energy Boundary Surface (PEBS) method [6]-[7], in combination with a time-domain simulation technique is employed. A fast hybrid training method is used for training the proposed RBF NN, and the method is applied to the 10-machine 39-bus New England test power system and the efficiency is examined. The rest of paper is organized as follows. Section 2 gives a brief introduction to the RBF neural network. Section 3 represents a general approach based on the PEBS method and the time-domain simulation technique for obtaining the ΔV_n. In Section 4, we propose our RBF neural network based method and introduce some case studies. Section 5 presents the simulation results, and Section 6 concludes the paper.

2. Radial Basis Function (RBF) Neural Network

Figure 1 shows a radial basis function (RBF) neural network. A radial basis function neural network has a hidden layer of radial units and a linear-output layer units. Similar to biological receptor fields, an RBF neural network employs local receptor fields to perform function mappings. In an RBF neural network, a radial unit (i.e., local receptor field) is defined by its center point and a radius. The activation function of the i-th radial unit is:

$$h_i = \mathrm{R}_i(\mathbf{x}) = R_i(\|\mathbf{x} - \mathbf{u}_i\| / \sigma_i) \qquad (1)$$

where $\mathbf{x}$ is the input vector, $\mathbf{u}_i$ is a vector with the same dimension as $\mathbf{x}$ denoting the center, σ is width of the function and $R_i(.)$ is the i-th radial basis function. Typically $R(.)$ is a Gaussian function:

$$R_i(\mathbf{x}) = \exp\left(\frac{\|\mathbf{x} - \mathbf{u}_i\|^2}{2\sigma_i^2}\right) \qquad (2)$$

The i-th component of the final output $\mathbf{y}$ of an RBF neural network can be computed as the weighted sum of the outputs of the radial units as:

$$y_i = \sum_i w_i R_i(\mathbf{x}) \qquad (3)$$

where w_i is the connection weight between radial unit i and the output unit.

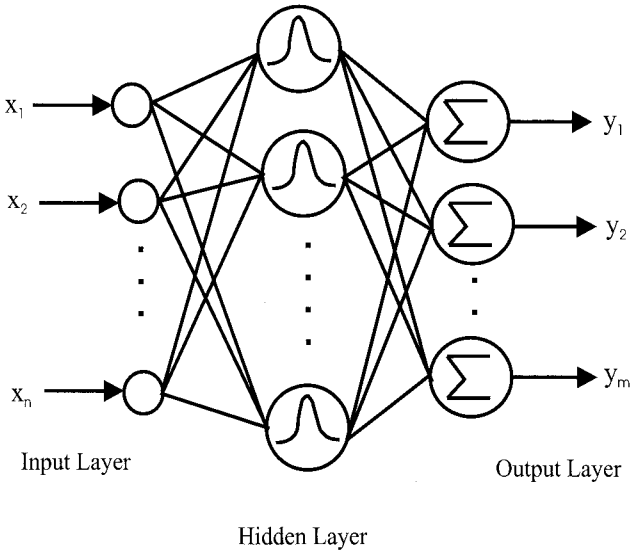

Fig. 1. A radial basis function (RBF) neural network

Training an RBF neural network is aimed at adjusting Gaussian basis function centers (u_i's) and spread (or width) parameters (σ_i's), and weights (w_i's) to result in minimum sum-squared error for all the output units among all the patterns [16]-[18]. In this paper, we used a hybrid (unsupervised/supervised) method for training the proposed RBF neural network. In unsupervised training phase of this hybrid method, we employed the Pao Euclidean distance-based clustering method [12]-[19] to select both the number of hidden neurons and the neuron centers. In this method, the input patterns are clustered according to the similarities discovered among the input features. The clustering process is governed by a threshold called the "vigilance" parameter and the Euclidian metric function. In the clustering, the first pattern is selected as the center of the first cluster. Then, the next pattern is compared with that of the first cluster center. If the distance is less than the vigilance parameter, it is clustered with the first. Otherwise, it is a center of a new cluster. This process is repeated for all patterns. Once all patterns are processed, the algorithm is reiterated until a stable cluster formation occurs. Then, the spreads are determined by a P-nearest neighbor method [20]. In supervised phase of this hybrid training method, the weights between the hidden and the output layers are computed directly using the pseudo-inverse technique.

3. Normalized Transient Energy Margin

With the usual notation, the mathematical model for an n-machine power system with constant voltage behind transient reactance representation and constant impedance load approximation is given in the Center of Inertia (COI) notation as [6]-[7], [21]:

$$\dot{\theta}_i = \tilde{\omega}_i$$

$$M_i\dot{\tilde{\omega}}_i = P_{mi} - P_{ei} - \frac{M_i}{M_T}P_{COI} \tag{4}$$

$$\hat{=} f_i(\theta) \quad i = 1,2,...,n \tag{5}$$

The right-hand side in equation (5) has different parameters (i.e., G_{ij} and B_{ij} values) in computing P_{ei} and P_{COI} for faulted period ($0 \le t \le t_{cl}$) and the post-fault period ($t > t_{cl}$). The energy function for the post-fault system is constructed as [6]-[7], [21]:

$$\begin{aligned} V(\theta,\tilde{\omega}) &= \frac{1}{2}\sum_{i=1}^{n} M_i\tilde{\omega}_i^2 - \sum_{i=1}^{n}\int_{\theta_i^s}^{\theta_i} f_i(\theta)d\theta_i \\ &= V_{KE}(\tilde{\omega}) + V_{PE}(\theta) \hat{=} V_{TOT} \end{aligned} \tag{6}$$

where θ_i and $\tilde{\omega}_i$ are the variables from the faulted trajectory. In the absence of transfer conductance terms $G_{ij}(i \neq j)$, the expression for $V_{PE}(\theta)$ can be expressed analytically in a closed form [6]-[7]. Otherwise the G_{ij} terms contribute a path dependent term as follows [22]:

$$V_{PE}(\theta) = -\sum_{i=1}^{n} P_i(\theta_i - \theta_i^s) - \sum_{i=1}^{n-1}\sum_{j=i+1}^{n}\left[C_{ij}(\cos\theta_{ij} - \cos\theta_{ij}^s) - I_{ij}\right] \tag{7}$$

where $C_{ij} = E_iE_jB_{ij}$, $D_{ij} = E_iE_jG_{ij}$, $P_i = P_{mi} - |E_i|^2 G_{ij}$, and I_{ij} is calculated as follows:

$$I_{ij} = \int_{\theta_i^s+\theta_j^s}^{\theta_i+\theta_j} D_{ij}\cos\theta_{ij}\, d(\theta_i + \theta_j)$$

In computing equation (7), θ_i is obtained from the faulted trajectory and θ_i^s is the post-fault stable equilibrium point. It is obvious that the third term of equation (7), i.e., I_{ij} is path dependent. In bulk of the literature, by assuming a straight line path of integration, the third term of equation (7) is approximated analytically as [21]:

$$I_{ij} = D_{ij}\frac{(\theta_i - \theta_i^s) + (\theta_j - \theta_j^s)}{(\theta_i - \theta_i^s) - (\theta_j - \theta_j^s)}(\sin\theta_{ij} - \sin\theta_{ij}^s) \tag{8}$$

As pointed out in [7], in all cases where the power system is stable following the removal of a disturbance, a certain amount of the total kinetic energy in the system is not absorbed. This clearly indicates that not all the transient kinetic energy, created by the disturbance, contributes to the instability of the system. Some of this kinetic energy is responsible for the inter-machine motion between the generators, and does not contribute to the separation of the severely disturbed generators from the rest of the system. Therefore, it is obvious that for accurate transient stability assessment using the TEF method, the component of kinetic energy not contributing to instability should be subtracted from the energy that needs to be absorbed by the system for stability to be maintained. In this paper, we have used the method presented in [7] to compute corrected Kinetic energy. If the system inertias are finite, the disturbance splits the generators of the system into two groups: the critical machines and the rest of the generators. Their inertial centers have inertia constants and angular speeds M_{cr} , $\tilde{\omega}_{cr}$, M_{sys} , $\tilde{\omega}_{sys}$, respectively. These parameters are obtained as follows:

$$M_{cr} = \sum_{i\in cr} M_i \,, M_{sys} = \sum_{i\in sys} M_i \tag{9}$$

$$\tilde{\omega}_{cr} = \frac{\sum_{i\in cr} M_i\tilde{\omega}_i}{M_{cr}} \,, \quad \tilde{\omega}_{sys} = \frac{\sum_{i\in sys} M_i\tilde{\omega}_i}{M_{sys}} \tag{10}$$

where the subscript "cr" denotes the critical machines group, while "sys" denotes the machines in the rest of the system. The kinetic energy causing the separation of the two groups is the same as that of an equivalent one-machine-infinite-bus system having inertia constant M_{eq} and angular velocity ω_{eq} given by:

$$M_{eq} = \frac{M_{cr}M_{sys}}{M_{cr} + M_{sys}} \tag{11}$$

$$\tilde{\omega}_{eq} = \left(\tilde{\omega}_{cr} - \tilde{\omega}_{sys}\right) \tag{12}$$

and the corresponding corrected kinetic energy is given by:

$$V_{KE_{corr}} = \frac{1}{2}M_{eq}\tilde{\omega}_{eq}^2 \tag{13}$$

Therefore, the kinetic energy term in equation (6) should be replaced by (13).

Computing two values of the transient energy makes the stability assessment feasible. The first value of the transient energy is normally determined at fault clearing time, V_{cl} . The other value denoted by V_{cr} , is the critical value of the transient energy function evaluated at the Controlling Unstable Equilibrium Point (CUEP), for the

particular disturbance under investigation. The system is stable (unstable), if $V_{cl} < V_{cr}$ ($V_{cl} > V_{cr}$). Due to complexity of exact computation of the CUEP, the evaluation of V_{cr} at the CUEP is a very hard task. In this paper, we have used the PEBS method for fast evaluation of V_{cr}. However, it has been shown in [7], [23] that the V_{cr} obtained by the PEBS method may be less or greater than its actual value. To remedy this drawback, the PEBS method along with a time-domain simulation technique of the system equations of motion is employed to obtain the actual value of V_{cr}.

Alternatively the transient stability assessment can be made by computing the transient energy margin ΔV given by:

$$\Delta V = V_{cr} - V_{cl} \tag{14}$$

If ΔV is greater than zero the system is stable, and if ΔV is less than zero, the system is unstable. Here, we have defined a normalized transient energy margin ΔV_n, which is suitable to be trained by neural networks. This normalized transient energy margin is calculated differently for stable and unstable cases as:

$$\Delta V_n = \begin{cases} \dfrac{V_{cr} - V_{cl}}{V_{cr}}, & \text{if system is stable } (t_{cr} > t_{cl}) \\ \dfrac{V_{cr} - V_{cl}}{V_{cl}}, & \text{if system is unstable } (t_{cr} < t_{cl}) \end{cases} \tag{15}$$

It can be easily shown that the value of ΔV_n lies between -1.0 and 1.0. If $\Delta V_n > 0$, the system is stable, and if $\Delta V_n < 0$, the system is unstable. This normalized transient energy margin represents a qualitative measure of the degree of stability (or instability) of the system. We have proposed the following procedure to compute the ΔV_n by using the PEBS method and the time-domain simulation technique:

Step 1- Integrate the faulted system dynamic equations until the transient potential energy reaches a maximum along the faulted trajectory. This maximum value denoted by V_{cr}^* provides a good estimate of actual V_{cr} [6].

Step 2- From the faulted trajectory find the time instant, t_{cr}^*, at which the transient energy V reaches V_{cr}^*. The t_{cr}^* is viewed as an estimate of actual t_{cr} [6].

Step 3- Find actual t_{cr} by using t_{cr}^* as an initial guess in the time-domain simulation technique accompanied by a trial-and-error method.

Step 4- Integrate the faulted system dynamic equations until time instant, $t = t_{cr}$. Find the value of system potential energy at this time instant. Also, find the system corrected kinetic energy using equation (13). Then, obtain the system critical energy V_{cr}, by adding the system potential and corrected kinetic energies.

Step 5- Integrate the faulted system dynamic equations until time instant, $t = t_{cl}$. Find the value of system potential energy at this time instant. Also, find the system corrected kinetic energy using equation (13). Then, obtain the system total energy at fault clearing time V_{cl}, by adding the system potential and corrected kinetic energies.

Step 6- Compute the system normalized transient energy margin ΔV_n, using equation (15).

4. The Proposed RBF Neural Network Methodology

In this section, we present our RBF neural network based approach by using the 10-machine 39-bus New England test system shown in Fig. 2. The system data are given in [6]. Although the method is being applied to this test system only, it is quite a general one and can be used for any other system in a similar manner. The objective of this study is to determine the normalized transient energy margin (ΔV_n) for three phase faults at two different locations. The first fault is applied at bus 26 and is cleared without removing any line in the post-fault system at 0.12 s after the fault. This fault is represented as fault 26*. The second fault is applied at bus 34 and is cleared by removing the line connected between bus 34 and bus 35 at 0.16 s after the fault. We represent this fault as fault 34*-35. Note that the faults are shown in Fig. 2.

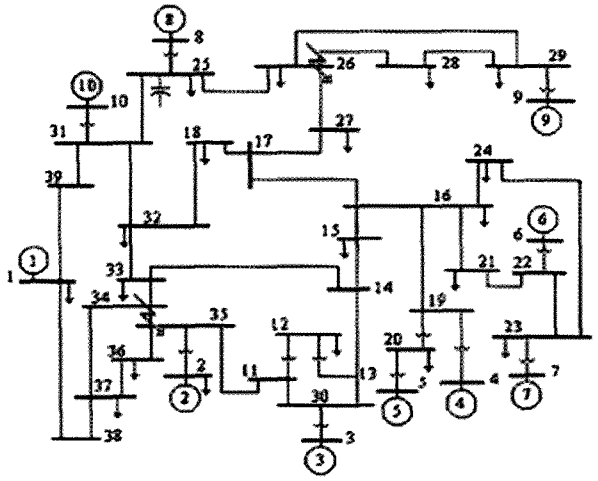

Fig. 2. One-line diagram of the New England test system

We know that the ΔV_n is a complex function of the pre-fault system operating point, fault type and location, and the post-fault system configuration. However, for a particular fault such as the faults mentioned above, the ΔV_n is indeed a function of only the pre-fault system operating point. The pre-fault operating point is determined by performing a load-flow analysis on the system by using an iterative numerical procedure. To perform a load-flow analysis, we need to provide the load-flow program some operating conditions along with the initial guesses for some unknown variables, such as the voltages of the PQ buses. The operating conditions, an independent set of variables that characterize the pre-fault system for a given topology, consist of the voltage magnitude and voltage angle of the slack bus, the voltage magnitudes and the generated active powers of the PV buses, and the active and reactive load powers of the PQ buses. The final values of the unknown variables, obtained by the load-flow analysis, are indeed the outputs of the load-flow program. It should be noted that these outputs are also functions of the independent operating conditions. These outputs are, respectively, the generated active and reactive powers of the slack bus, the generated reactive powers and voltage angles of the PV buses, and the voltage magnitudes and voltage angles of the PQ buses.

As shown in Fig. 3, the independent operating conditions along with all the outputs of the load-flow program are given to the transient stability program and this program calculates the ΔV_n. As mentioned above, all the outputs of the load-flow program are functions of the independent operating conditions. Therefore, the output of the transient stability program (i.e., ΔV_n), is indeed a function of the independent operating conditions. Moreover, an RBF neural network can be directly employed for approximation of the function (refer Fig. 3).

We have already shown that the ΔV_n is a function of an independent set of operating conditions in the pre-fault system. We now want to present these operating conditions in the New England test system. Here, we

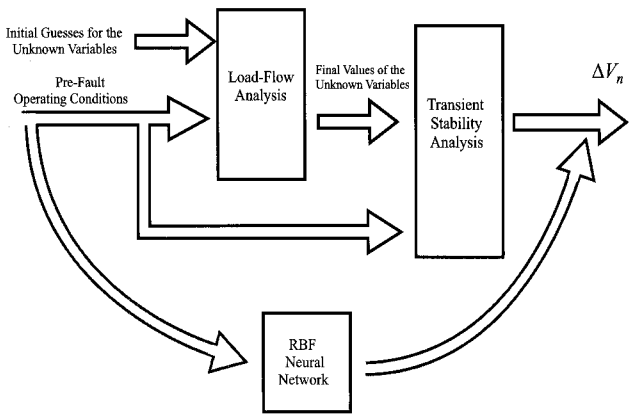

Fig. 3. A conceptual diagram of the proposed method

assume that bus 1 represents the slack bus. The remaining generation buses (i.e., buses 2-10) are considered as PV buses, which their generated active powers and voltage magnitudes are denoted by PG_i and V_i (i=2,3, ... ,10). Besides one slack bus and 9 PV buses, the test system consists of an additional 29 PQ buses (i.e., buses 11-39). However, the loads are acting only on 19 distinct buses. The active and reactive load powers of these buses are denoted by PD_j and QD_j (j is the bus number). Note that the shunt capacitor installed at bus 25 is treated as a load, which its generated reactive power is known as Q_c.

Without loss of generality, it is assumed that the voltage magnitude and voltage angle of the slack bus (i.e., bus 1) are fixed at their assumed specified values. Therefore, all the independent operating conditions in the New England test system are:

- Voltage magnitudes of all the 9 PV buses ($V_2 - V_{10}$)
- Generated active powers of all the 9 PV buses ($PG_2 - PG_{10}$)
- Active load powers of all the 19 loads acting on different buses ($PD_1, PD_2, ..., PD_{37}$)
- Reactive load powers of all the 19 loads acting on different buses ($QD_1, QD_2, ..., QD_{37}$)
- Generated reactive power of the single shunt capacitor installed at bus 25 (Q_c)

Therefore, for a particular fault scenario, the ΔV_n is a function of the above (9+9+19+19+1) =57 independent operating conditions. To approximate this function with an RBF neural network is the main objective of this paper. For this purpose, the proposed RBF neural network needs to be trained on a limited set of cases covering the operating conditions for the test system. Once the training of the RBF neural network is completed, the ΔV_n can be quickly computed. Because, all the 57 operating conditions are, in general, directly measured in an energy control center (ECC). However, it is necessary to develop a set of neural networks for a set of fault scenarios for the study system, because a different training data set for ΔV_n is needed for each contingency. As it is shown in Fig. 4, the inputs of all of these neural networks are the same so that the neural networks operate in parallel during testing. Thus, the overall recall time of the proposed system is quite small.

The procedure for obtaining the training or testing data patterns is composed of the following steps:

1) The minimum and maximum limits of the generated reactive powers in all the PV buses are set to -0.2 and 0.7 times their nominal generated active powers, respectively.

2) It is assumed that the following operating conditions vary independently over some specified ranges:

   (a) Voltage magnitudes of all the 9 PV buses
   (b) Generated active powers of all the 9 PV buses
   (c) Active and reactive powers of all the 19 loads
   (d) Generated reactive power of the shunt capacitor located at bus 25

   It is further assumed that the range of variations of the voltage magnitudes of PV buses is bounded to 0.9 to 1.1 times their corresponding nominal values. The range of variations of the other operating conditions is bounded to 0.6 to 1.1 times their corresponding nominal values.

3) A random value with uniform distribution is assigned independently to each of the variables mentioned in step 2.

4) With the above-prepared data, an AC load-flow is performed. The results may show that some PV buses may be treated as PQ buses. However, the voltage magnitudes of all the violated and non-violated PV buses are used as the inputs of the proposed neural network.

5) The method proposed in Section 3 is employed to calculate the ΔV_n.

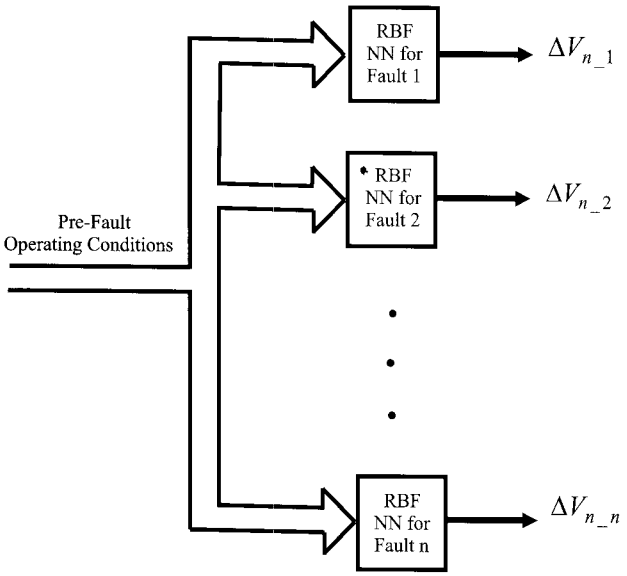

Fig. 4. A parallel neural networks operation for all faults

Here, we have assumed that the reactive power generation limits of the PV buses are fixed for all operating conditions, and therefore these limits have not been chosen as the inputs of the proposed NN. If these limits are changed, we can use them as the additional inputs of the proposed neural network.

5. The Simulation Results

The proposed RBF neural network based method was applied to the 10-machine 39-bus New England test system. This section presents the simulation results. The simulation results for the fault 26* are first presented here. With the procedure presented in Section 4, a database of 3000 operating conditions was built from which 2000 cases were chosen for training and the remaining 1000 cases for testing of the proposed RBF NN (see Fig. 3).

As mentioned in Section 2, we used a hybrid (unsupervised/supervised) method for training the RBF neural network. In unsupervised training phase of this hybrid method, we employed the Euclidean distance-based clustering method [12], [19]. The clustering process is controlled by a threshold called vigilance parameter. If the Euclidean distance between two input vectors is less than the vigilance parameter, they are included in the same cluster. By employing this clustering method with different values for the vigilance parameter, we came up with different number of hidden neurons for the RBF NN. In each case, after finding the structure of the RBF NN and its parameters, the trained NN was tested using testing data patterns. The performance of the trained NN was examined by the Root Mean-Squared (RMS) error between the actual and the estimated normalized transient energy margin (ΔV_n).

The training time of the proposed RBF neural network and the RMS error for testing patterns are shown in Fig. 5 versus the vigilance parameter. It can be seen from this figure that the RMS error initially decreases and finally reaches to a minimum value as the value of the vigilance parameter is decreased. The minimum value of RMS error was found to be 0.075. In unsupervised training phase of the RBF neural network, 3 iterations were performed to form a stable cluster with the vigilance parameter equal to 2.7. Total elapsed time for training the RBF network was 240 seconds on a Pentium IV 2.4 GHz with 512 MB of RAM.

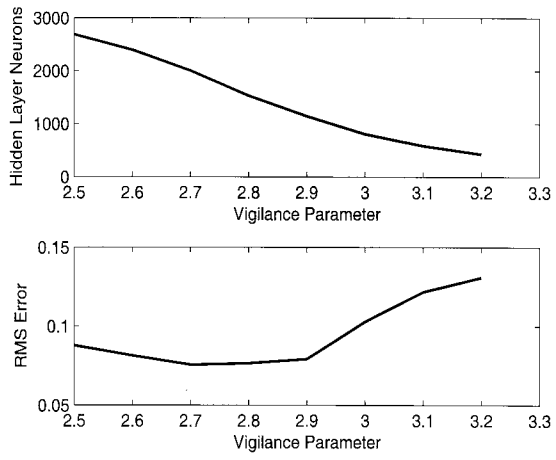

Fig. 5. The number of hidden neurons and RMS error of test patterns versus the vigilance parameter for fault 26*

The obtained value of the RMS error for testing patterns (i.e., 0.075) proves the generalization accuracy of the trained RBF neural network for the fault 26*. To see this better, Fig. 6 compares the actual and the estimated ΔV_n for 50 out of 1000 testing patterns. It can be seen from this figure that the trained RBF neural network can estimate the actual ΔV_n with a good degree of accuracy.

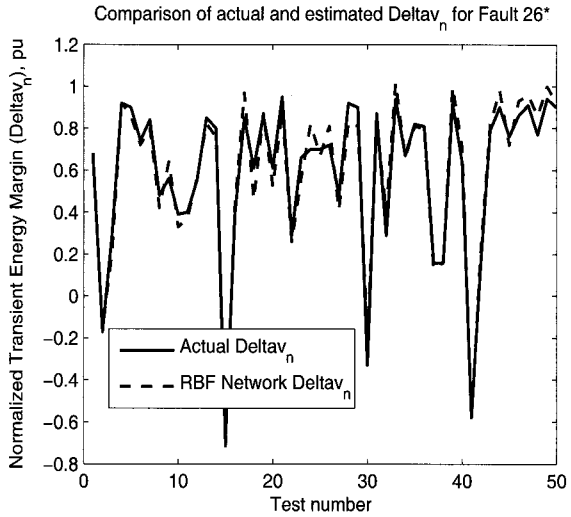

Fig. 6. Comparison of the actual and estimated ΔV_n for fault 26* using an RBF NN

Similar results were obtained for the fault 34*-35 using another RBF neural network. In this case, the minimum value for RMS error of testing patterns was found to be 0.102, proving the generalization accuracy of the trained RBF neural network for fault 34*-35 too. To see this better, Fig. 7 compares the actual and the estimated ΔV_n for 50 out of 1000 testing patterns. It can be seen from this figure that the trained RBF neural network can estimate the actual transient energy margin with a good degree of accuracy.

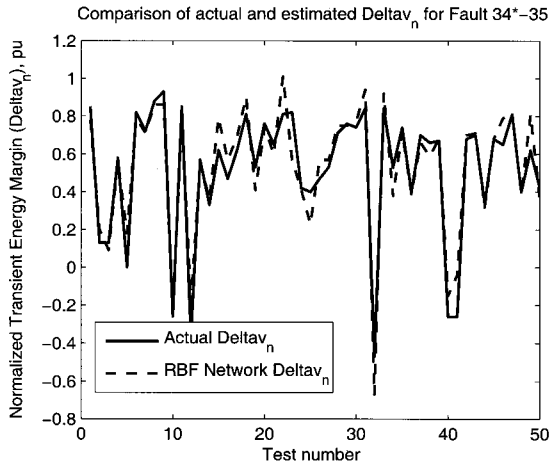

Fig. 7. Comparison of the actual and estimated ΔV_n for fault 34*-35 using an RBF NN

It is worth mentioning here that the obtained values for testing RMS error are acceptable in practical applications. Because, the ΔV_n represents a qualitative measure of the degree of stability (or instability) of the system.

We know that the power system topology is being changed due to transmission lines or generators outages. In these cases, the trained RBF neural network for a specific topology will be failed to estimate the accurate results for the ΔV_n as it would be unable to capture the inputs-outputs relationship properly. A solution for this problem is to train a separate RBF neural network for each possible system topology. Another solution is to use the transmission lines or generators status as the additional inputs for the proposed RBF neural network. Using the above aspects in a power system, therefore, present directions for further research.

6. Conclusion

A radial basis function (RBF) neural network (NN) based approach was proposed for the on-line transient stability analysis (TSA) of power systems through a normalized transient energy margin (ΔV_n) estimation for a particular contingency under different operating conditions. The inputs of the proposed RBF neural network were an independent set of directly measurable conditions, which characterize the pre-fault system. Simulation results using the New England test power system indicated that the trained RBF neural network could be employed to estimate the ΔV_n with a good degree of accuracy. The RBF neural network required an iterative procedure for clustering the data to determine the number of hidden (RBF) nodes. A fast hybrid method was used for training the RBF neural network. First, the Euclidean distance-based clustering technique was employed to select both the number of hidden neurons and neuron centers. Then, weights between the hidden and output layers were computed directly using the pseudo-inverse technique. The general conclusion is that the proposed approach is well suitable for on-line normalized transient energy margin estimation because of the accuracy and computational efficiency.

Acknowledgements

The author would like to acknowledge the financial support provided by University of Guilan in Iran.

References

[1] L.L. Grigsby, *Power System Stability and Control*: CRC Press, 2007.

[2] IEEE/CIGRE Joint Task Force, "Definition and Classification of Power System Stability", *IEEE Trans. Power Systems*, Vol. 1, No. 2, 2004.

[3] A.L. Bettiol, A. Souza, J.L. Todesco, and J.R Tesch, "Estimation of Critical Clearing Times Using Neural Network", *in Proceedings of IEEE Bologna PowerTech Conference*, Bologna, Italy, 2003.

[4] P. Kundur, *Power System Stability and Control*: McGraw-Hill, 1994.

[5] M. Pavella and P.G. Murthy, *Transient Stability of Power Systems: Theory and Practice*: John Wiley, 1994.

[6] M.A. Pai, *Energy Function Analysis for Power System Stability*: Kluwer Academic, 1989.

[7] A.A. Fouad and V. Vittal, *Power System Transient Stability Analysis Using the Transient Energy Function Method*: Prentice-Hall, 1992.

[8] Y. Xue, T.V. Cutsem, and M. Pavella, "Extended Equal Area Criterion Justifications, Generalizations, Applications", *IEEE Trans.Power Systems*, Vol. 4, pp. 44-52, 1989.

[9] Y. Xue, T.V. Cutsem, and M. Pavella, "A Simple Direct Method for Fast Transient Stability Assessment of Large Power Systems", *IEEE Trans.Power Systems*, Vol. 3, pp. 400-412, 1998.

[10] D.J. Sobajic and Y.H. Pao, "Artificial Neural-Net Based Dynamic Security Assessment for Electric Power Systems", *IEEE Trans. Power Systems*, Vol. 4, No. 1, pp. 220-226, 1989.

[11] M. Djukanovic, D.J. Sobajic, and Y.H. Pao, "Neural-Net Based Unstable Machine Identification Using Individual Energy Functions", *Int. Journal of Electrical Power and Energy Systems*, Vol. 13, No. 5, pp. 255-262, 1991.

[12] Y.H. Pao and D.J. Sobajic, "Combined Use of Unsupervised and Supervised Learning for Dynamic Security Assessment", *IEEE Trans. Power Systems*, Vol. 7, No. 2, pp. 878-884, 1992.

[13] Q. Zhou, J. Davidson, and A.A. Foaud, "Application of Artificial Neural Networks in Power System Security and Vulnerability Assessment", *IEEE Trans. Power Systems*, Vol. 9, No. 1, pp. 525-532, 1994.

[14] E. Hobson and G.N Allen, "Effectiveness of Artificial Neural Networks for First Swing Stability Determination of Practical Systems", *IEEE Trans. Power Systems*, Vol. 9, No. 2, pp. 1062-1068, 1994.

[15] F. Aboytes and R. Ramirez, "Transient Stability Assessment in Longitudinal Power Systems Using Artificial Neural Networks", *IEEE Trans. Power Systems*, Vol. 11, No. 4, pp. 2003-2010, 1996.

[16] A.G. Bahbah and A.A. Girgis, "New Method for Generators' Angles and Angular Velocities Prediction for Transient Stability Assessment of Multimachine Power Systems Using Recurrent Artificial Neural Network", *IEEE Trans. Power Systems*, Vol. 19, No. 2, pp. 1015-1022, 2004.

[17] T. Chen, and H. Chen, "Approximation Capability to Functions of Several Variables Nonlinear Functional, and Operators by Radial Basis Function Neural Network", *IEEE Trans. Neural Networks*, Vol. 6, pp. 904-910, 1995.

[18] S. Haykin, *Neural Networks: A Comprehensive Foundation*, Second Edition: Prentice-Hall, 1999.

[19] T. Jain, L. Srivastava, and S.N. Singh, "Fast Voltage Contingency Screening Using Radial Basis Function Neural Network", *IEEE Trans. Power Systems*, Vol. 18, No. 4, pp. 359-1366, 2003.

[20] N.B. Karayiannis and G.W. Mi, "Growing Radial Basis Neural Networks: Merging Supervised and Unsupervised Learning with Network Growth techniques", *IEEE Trans. Neural Networks*, Vol. 8 No. 6, pp. 1492-1506, 1997.

[21] M.A. Pai, M. Laufenberg, and P.W. Sauer, „Some Clarifications in the Transient Energy Function Method", *International Journal of Electrical Power & Energy Systems*, Vol. 18, No. 1, pp. 65-72, 1996.

[22] T. Athay, R. Podmore, and S. Virmani, "A Practical Method for Direct Analysis of Transient Stability" *IEEE Trans. Power Systems*, Vol. 98, No. 2, pp. 573-584, 1979.

[23] H.D. Chiang, F.F. Wu, and P. Varaiya,, "Foundation of the Potential Energy Boundary Surface Method for Power System Transient Stability Analysis", *IEEE Trans. Circuits and Systems*, Vol. 35, No. 6, pp. 712-728, 1988.

Ali Karam

He is an Assistant Professor at University of Guilan in Iran. He received B.S. at Sharif University of Technology, Tehran, in 1992, M.S. at Iran University of Science and Technology, Tehran, in 1994 and Ph.D. at Amirkabir University of Technology (Tehran Polytechnic) in 1999 all in electrical engineering. His research interests include transient stability, transient energy function method and neural network applications.